Received: 29 May 2018 | Accepted: 19 June 2018

DOI: 10.1111/gcb.14400

PRIMARY RESEARCH ARTICLES

WILEY Global Change Biology

A radiative forcing analysis of tropical peatlands before and after their conversion to agricultural plantations

René Dommain[1,2,*] | Steve Frolking[3,*] | Aurich Jeltsch-Thömmes[4] | Fortunat Joos[4] | John Couwenberg[5] | Paul H. Glaser[6]

[1]Institute of Earth and Environmental Science, University of Potsdam, Potsdam, Germany

[2]Department of Anthropology, Smithsonian Institution, National Museum of Natural History, Washington, District of Columbia

[3]Institute for the Study of Earth, Oceans, and Space, University of New Hampshire, Durham, New Hampshire

[4]Climate and Environmental Physics, Physics Institute and Oeschger Centre for Climate Change Research, University of Bern, Bern, Switzerland

[5]Institute of Botany and Landscape Ecology, Partner in the Greifswald Mire Center, University of Greifswald, Greifswald, Germany

[6]Department of Earth Sciences, University of Minnesota, Minneapolis, Minnesota

Correspondence
René Dommain, Institute of Earth and Environmental Science, University of Potsdam, 14476 Potsdam, Germany.
Email: dommain@uni-potsdam.de

Funding information
European Social Fund, Grant/Award Number: ESF/14-BM-A55-0030/16; Ministry of Education, Science and Culture of Mecklenburg-Western Pomerania, Grant/Award Number: WETSCAPES; USDA, Grant/Award Number: 10JV11242306135; Schweizerischer Nationalfonds zur Förderung der Wissenschaftlichen Forschung, Grant/Award Number: 200020_172476; Geo.X; NASA, Grant/Award Number: NNX14AD31G

Abstract

The tropical peat swamp forests of South-East Asia are being rapidly converted to agricultural plantations of oil palm and *Acacia* creating a significant global "hot-spot" for CO_2 emissions. However, the effect of this major perturbation has yet to be quantified in terms of global warming potential (GWP) and the Earth's radiative budget. We used a GWP analysis and an impulse-response model of radiative forcing to quantify the climate forcing of this shift from a long-term carbon sink to a net source of greenhouse gases (CO_2 and CH_4). In the GWP analysis, five tropical peatlands were sinks in terms of their CO_2 equivalent fluxes while they remained undisturbed. However, their drainage and conversion to oil palm and *Acacia* plantations produced a dramatic shift to very strong net CO_2-equivalent sources. The induced losses of peat carbon are ~20× greater than the natural CO_2 sequestration rates. In contrast, a radiative forcing model indicates that the magnitude of this shift from a net cooling to warming effect is ultimately related to the size of an individual peatland's carbon pool. The continuous accumulation of carbon in pristine tropical peatlands produced a progressively negative radiative forcing (i.e., cooling) that ranged from −2.1 to −6.7 nW/m^2 per hectare peatland by 2010 CE, referenced to zero at the time of peat initiation. Peatland conversion to plantations leads to an immediate shift from negative to positive trend in radiative forcing (i.e., warming). If drainage persists, peak warming ranges from +3.3 to +8.7 nW/m^2 per hectare of drained peatland. More importantly, this net warming impact on the Earth's radiation budget will persist for centuries to millennia after all the peat has been oxidized to CO_2. This previously unreported and undesirable impact on the Earth's radiative balance provides a scientific rationale for conserving tropical peatlands in their pristine state.

KEYWORDS
Acacia plantation, CO_2 emissions, drainage-based land use, global warming potential, oil palm plantation, radiative forcing, tropical peatland

1 | INTRODUCTION

Terrestrial ecosystems play a critical role in influencing the radiative balance of the Earth (e.g., Field, Lobell, Peters, & Chiariello, 2007; Foley, Costa, Delire, Ramankutty, & Snyder, 2003; IPCC 2013) and thus global average temperatures (Myhre et al., 2013). However, determining the contributions of specific ecosystems to the radiative budget, and the radiative impact of human alterations of terrestrial ecosystems, remains a major challenge (Bonan, 2008; Le Quéré

*These authors contributed equally to this article.

et al., 2018). Peatland ecosystems affect the climate system by continuously sequestering carbon in thick organic deposits over millennia, representing persistent long-term carbon dioxide (CO_2) sinks (Dommain, Couwenberg, Glaser, Joosten, & Suryadiputra, 2014; Frolking & Roulet, 2007; Gorham, 1991; Kleinen, Brovkin, von Bloh, Archer, & Munhoven, 2010). Peatlands also emit globally significant amounts of methane (CH_4), a potent greenhouse gas (Frolking et al., 2011; Kirschke et al., 2013) that is produced by anaerobic microbial decomposition from simple carbon substrates (e.g., Glaser & Chanton, 2009).

Over 10% of the global peatland area is found in the tropical belt, with 250,000 km^2 peatlands in equatorial South-East Asia alone (Page, Rieley, & Banks, 2011). These peatlands store an estimated 70 Pg C (Page et al., 2011), which has accumulated at the high average rate of ~70 g C m^{-2} $year^{-1}$ during the Holocene epoch (Dommain, Couwenberg, & Joosten, 2011). South-East Asian peatlands are naturally covered by peat swamp forests, but are now being rapidly logged and converted into drained agricultural production areas, mainly for oil palm and *Acacia* pulpwood cultivation (Dommain et al., 2016). By 2015 nearly 30% of the peatlands in Borneo, Sumatra and Peninsular Malaysia had been converted to industrial plantations comprising 3.1 million ha of oil palm and 1.1 million ha of *Acacia* pulp (Miettinen, Shi, & Liew, 2016).

Tropical peatland plantations require artificial drainage networks that lower the water table by about 50–80 cm (e.g., Hooijer et al., 2012), producing a thick aerobic zone in which decomposition releases about 5–10 kg CO_2 m^{-2} $year^{-1}$ (Carlson, Goodman, & May-Tobin, 2015; Couwenberg, Dommain, & Joosten, 2010; Couwenberg & Hooijer, 2013; Hooijer et al., 2012; Jauhiainen, Hooijer, & Page, 2012a; Khasanah & van Noordwijk, 2018). It has been estimated that aerobic peat decomposition from drained agricultural plantation areas in South-East Asia now generates emissions of between about 380 and 420 Tg CO_2 $year^{-1}$ (Dommain et al., 2016; Miettinen, Hooijer, Vernimmen, Liew, & Page, 2017). Moreover, widespread drainage associated with the expansion of these plantations has facilitated the spread of catastrophic peat fires (Gaveau et al., 2014), which emit additional carbon to the atmosphere. Consequently, drained South-East Asian peatlands are now a global hot-spot for anthropogenic carbon emissions (Couwenberg et al., 2010; Dommain et al., 2016; Hooijer et al., 2010; Page & Hooijer, 2016; Van der Werf et al., 2009). However, the radiative forcing effect of these globally significant carbon emissions has not been quantified. Two approaches are currently available to calculate the potential impact of peatland conversions on the global climate system: global warming potential metrics and radiative forcing analysis.

1.1 | Global warming potential metrics

Global warming potential (GWP) metrics are commonly used to convert pulse fluxes of nonCO_2 greenhouse gases into CO_2-equivalents (CO_{2eq}) in terms of their radiative impact with respect to the same mass of CO_2 emitted over a specific, but arbitrary, time horizon. The typical time horizons used are 20, 100, or 500 years (Bridgham, Moore, Richardson, & Roulet, 2014; Forster et al., 2007; Myhre et al., 2013). Pulse-based GWP values are used in national reporting to the United Nations Framework Convention on Climate Change (UNFCCC) and commonly cover multiple gas species in peatland studies (e.g., Friborg, Soegaard, Christensen, Lloyd, & Panikov, 2003; Roulet, 2000; Whiting & Chanton, 2001; Wilson et al., 2016). GWP values have also been reported for tropical peat swamp forests in which they have been inappropriately based on total soil CO_2 fluxes, not net ecosystem CO_2 fluxes (Couwenberg et al., 2010).

1.2 | Radiative forcing

Taking the nonpulse character of the fluxes into account, the other method uses a simple impulse-response or force-restore representation of atmospheric perturbations to compute the radiative forcing (RF) impact over time due to net CO_2 and CH_4 fluxes (Neubauer & Megonigal, 2015). The lifetime of a CO_2 perturbation in the atmosphere is best represented by multiple lifetimes (e.g., Joos et al., 1996, 2013) because carbon cycles through several Earth system reservoirs with vastly different residence times. The CO_2 burden response of the atmosphere can then be approximated by a set of noninteracting linear exchanges of different lifetimes (Joos et al., 1996, 2013). Here, we use an empirical approximation to compute the impact of peatland CO_2 (and CH_4) fluxes (Figure 1). This approach has been applied to land-cover change of a boreal peatland (Lohila et al., 2010), drainage of a boreal peatland (Minkkinen, Korhonen, Savolainen, & Laine, 2002), Holocene C accumulation in northern peatlands collectively (e.g., Frolking & Roulet, 2007), and Holocene development of a subarctic fen (Mathijssen et al., 2014). Petrescu et al. (2015) used a hybrid approach to synthesize peatland climate impacts by determining the set of constant CO_2 and CH_4 fluxes that produce no net integrated radiative forcing over 20 or 100 years in order to classify northern and temperate peatlands relative to those "equilibrium" fluxes.

1.3 | Objectives of this study

Drained tropical peatlands have previously been reported to have lower global warming potentials than natural peat swamp forests, and these land-use conversions have therefore been considered unharmful in terms of global warming (e.g., Inubushi & Hadi, 2007; Melling, 2013; Melling, Hatano, & Goh, 2005a,b). We will rebut this contention by determining GWPs for tropical peatlands in both a natural and drained state, while also quantifying the radiative forcing impact of tropical peatland drainage. The main objectives of this study are therefore to (a) quantify the atmospheric CO_2 and CH_4 burdens, radiative forcing, and global warming potential of CO_2 and CH_4 fluxes from tropical peatlands under pristine naturally forested conditions, (b) determine the impact on these variables after peatland conversion to drained oil palm and *Acacia* plantations, and (c) compare these impacts from tropical peatlands to a well-studied representative northern peatland.

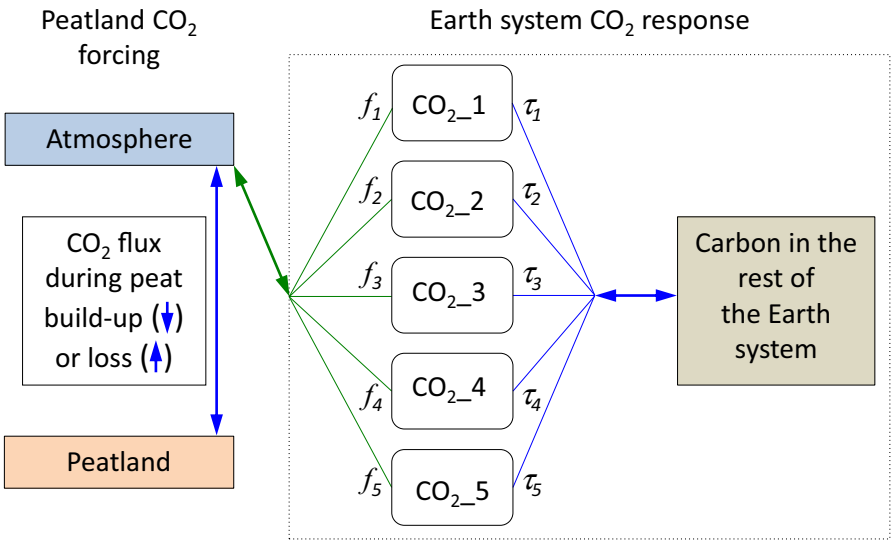

FIGURE 1 Atmospheric CO_2 perturbation model (Equation 1). The atmospheric CO_2 perturbation is represented by five noninteracting reservoirs (CO_2_i) with first-order perturbation lifetimes (τ_i). While peat is accumulating (preconversion), CO_2 flux into peatland is removed from the five-first-order, noninteracting atmospheric reservoirs at proportions (f_i). The rest of the Earth system delivers CO_2 to those five pools, causing them to approach or reach a negative steady-state value for constant peat uptake at their characteristic lifetimes (τ_i). While peat is decomposing (postconversion), CO_2 flux out of the peatland is added to the five-first-order, noninteracting atmospheric reservoirs at proportions (f_i), and the rest of the Earth system eventually removes CO_2 from those five pools causing them to approach or reach a positive steady-state value at their characteristic response times (τ_i). Once the peat has all been oxidized, the peatland forcing goes to zero, and the Earth system removes CO_2 from the atmosphere, eventually bringing the perturbation of all five reservoirs to zero in accord with their characteristic lifetimes (τ_i). See Table 3 for f_i and τ_i parameter values. Though not shown in this figure, atmospheric CH_4 perturbation (Equation 2) is represented by a single pool (see Table 3). Following the convention of IPCC for radiative forcing calculations, methane oxidation in the atmosphere is not counted as an input to atmospheric CO_2 (Myhre et al., 2013)

2 | MATERIALS AND METHODS

2.1 | Sites, land-use conversion scenarios, and greenhouse gas fluxes

We analyzed five tropical peat swamp forest sites in South-East Asia that have been recently drained and converted to plantations (Table 1, Supporting Information Figure S1). For comparison, we also include the well-studied Mer Bleue bog, an undisturbed northern raised bog in Ontario, Canada (Roulet et al., 2007). All five tropical sites, except for the Merang peatland, have had their basal peat dated, and their record of peat–carbon accumulation (i.e., CO_2 uptake) calculated from radiocarbon-dated peat cores (Supporting Information Table S1). The age of the Merang site was estimated by the transfer function approach outlined in Dommain et al. (2014), whereas its average rate of carbon accumulation was estimated from that reported for coastal Sumatran peatlands (Dommain et al., 2014).

Few data exist on CH_4 emissions from pristine tropical peat swamp forests, and none for the five tropical sites included in this study. We therefore calculated an average value for methane emissions (2.25 g CH_4 m^{-2} $year^{-1}$) using flux data (n = 69, including tree-mediated flux) from natural peat swamp forests measured at water table elevations of +20 cm to −20 cm relative to the peat surface (Couwenberg et al., 2010; Hatano et al., 2011; Pangala, Moore, Hornibrook, & Gauci, 2013; Melling, Goh, Kloni, & Hatano, 2012; Supporting Information Figure S2). For the Mer Bleue site, we used a CO_2 uptake and CH_4 emission paleoreconstruction provided by Nigel Roulet (personal communication), based on field measurements (e.g., Moore et al., 2011; Roulet et al., 2007) and peat core analyses (Frolking et al., 2010). Carbon dioxide uptake declined from 0.29 during the initial fen phase to 0.075 kg CO_2 m^{-2} $year^{-1}$ during the bog phase, and similarly, CH_4 emission declined from 0.0175 to 0.0065 kg CH_4 m^{-2} $year^{-1}$ over the ca. 8,000 years of the peatland's development (Supporting Information Section S.1).

For drained and converted tropical peatlands, we use representative CO_2 emission rates for typical drainage depths maintained in oil palm (−60 cm, 6,600 g CO_2 m^{-2} $year^{-1}$; Couwenberg & Hooijer, 2013) and *Acacia* plantations (−80 cm, 8,000 g CO_2 m^{-2} $year^{-1}$; Jauhiainen et al., 2012a; Table 2). For plantations we combined average methane emissions from surface flux data (oil palm: Couwenberg et al., 2010; Melling et al., 2012; *Acacia*: Hatano et al., 2011; Sumawinata, Suwardi, & Munoz, 2012; Jauhiainen, Hooijer, & Page, 2012b; see Table 2, and Supporting Information Figure S2) with CH_4 emissions from drainage ditches in plantations (Jauhiainen & Silvennoinen, 2012). The CH_4 emissions were computed per hectare as the area-weighted average of peat soil and drainage ditch fluxes (cf. Drösler et al., 2014; Table 2). The percent area occupied by ditches was determined from analysis of high-resolution Google Earth Pro™ satellite images of drained plantation areas (Supporting Information Section S.2; Figure S3).

TABLE 1 Study sites, location, peat depth, basal age, mean CO_2 uptake, and CH_4 emission before land-use conversion. See supplemental material for more details on peat carbon accumulation rates. All values reported to two significant figures

Site (region, country)	Marudi (Sarawak, Malaysia)	Rasau Jaya (W. Kalimantan, Indonesia)	Lower Baram Delta (Sarawak, Malaysia)	Siak Kanan (Riau, Indonesia)	Merang (South Sumatra, Indonesia)	Mer Bleue (Ontario, Canada)
Location	4°10′N, 114°15′E	0°14′S, 109°25′E	4°31′N, 114°5′E	0°52′N, 102°8′E	1°57′S, 103°55′E	45°24′N, 75°30′W
Peat depth at conversion (m)	12	7.0	2.2	9.9	3.0	5.0
Age (basal date) (years BP)	4,800	4,200	1,500	5,100	1,700	8,000
CO_2 uptake rate (g CO_2 m^{-2} $year^{-1}$)	400	270	240	270	285	140
Mean CH_4 emission rate (g CH_4 m^{-2} $year^{-1}$)	2.3	2.3	2.3	2.3	2.3	10
Total peat C in 2010 CE (Mg C ha^{-1})	5,300	3,100	1,000	3,800	1,300	3,000
Land-use conversion	Oil palm	Oil palm	Oil palm	*Acacia*	*Acacia*	NA
Years to lose all peat	290	170	60	170	52	NA

TABLE 2 CO_2 and CH_4 fluxes after land-use conversion

	Oil palm	*Acacia*
CO_2 loss rate postconversion (g CO_2 m^{-2} $year^{-1}$)	6,600	8,000
Peat soil CH_4 emission rate postconversion (g CH_4 m^{-2} $year^{-1}$)	0.003	0.22
Ditch CH_4 emission rate postconversion (g CH_4 m^{-2} $year^{-1}$)	320	320
Proportion of ditch area per ha	3.7	4.3
Area-weighted CH_4 emission postconversion (g CH_4 m^{-2} $year^{-1}$)	12	14

For the tropical peat swamp forest sites, we include a regional mean estimate of 170 Mg C ha^{-1} for the substantial aboveground biomass that existed on these sites prior to their conversion to plantations (Verwer & van der Meer, 2010). For the impulse-response function modeling (see below) we assume this biomass accumulates over the first 170 years of peatland development at a rate of 1 Mg C ha^{-1} $year^{-1}$, which we add to the peat C accumulation rate. We then apply the simplifying assumption that this aboveground biomass C remains constant until it is lost in the first year of land conversion to oil palm or *Acacia*, by adding this biomass to the peat C loss rate resulting from drainage. For the temperate Mer Bleue Bog, dominated by ericaceous shrubs and *Sphagnum* moss, we assume an aboveground biomass of 3 Mg C ha^{-1} (Moore, Bubier, Frolking, Lafleur, & Roulet, 2002) that accumulates at a rate of 0.1 Mg C ha^{-1} $year^{-1}$ over the first 30 years of peatland development. The Mer Bleue site has not been altered by land-use conversion.

2.2 | Global warming potentials

For all three land-use types, we calculated global warming potentials over 20, 100, and 500-year time horizons (denoted GWP_{20}, GWP_{100}, GWP_{500}). We calculated GWP for natural conditions before conversion based on the average carbon uptake rate for the most recently dated interval, that is, between the uppermost radiocarbon date and the peat surface (Supplemental Table S1). For CH_4, we used GWP values of 86 and 34 kg CO_{2eq} kg^{-1} CH_4 for the 20- and 100-year time horizons (Myhre et al., 2013). The 500-year time horizon GWP value for CH_4 is not provided by Myhre et al. (2013) so we used a value derived from our radiative forcing analysis (8.2 kg CO_{2eq} kg^{-1} CH_4; see below). In the calculations of GWPs, we did not consider nitrous oxide emissions because there are insufficient long-term flux data to estimate annual fluxes from tropical peatland systems for this episodically released gas.

2.3 | Impulse-response model of atmospheric CO_2 and CH_4 perturbations

2.3.1 | Computing atmospheric perturbations due to peatland net gas fluxes

We simulated the peatland radiative forcing impact using impulse-response functions (Joos et al., 2013) to represent the perturbation to an otherwise constant atmosphere due to net peatland CO_2 and CH_4 fluxes. This approach approximates the Earth system response to a greenhouse gas flux perturbation by representing the behavior of the rest of the Earth system as a set of noninteracting, first-order responses characterized by constant lifetimes (Figure 1). A constant or time-varying net CO_2 flux (emission or uptake), $\Phi_{CO2}(t')$, since an arbitrary start time, $t = 0$, produces a perturbation to the atmospheric CO_2 burden at any time t that is given by

$$CO_2(t) = \sum_{i=1}^{5}\left(f_i \cdot \int_0^t \Phi_{CO_2}(t')e^{(t'-t)/\tau_i}dt'\right) \quad (1)$$

where f_i is the fraction of the flux added to (if net emission) or removed from (if net uptake) CO_2 reservoir i, which has a lifetime of τ_i. The parameterization of Equation 1 (see Table 3) was developed by fitting the model response to the carbon cycle behavior of Earth System Models (Joos et al., 2013). We use a modification of the mean model parameter values reported by Joos et al. (2013) to account for millennial timescale responses. This mean model was based on fitting Equation 1, with only four CO_2 pools, to the carbon cycle dynamics of

TABLE 3 Impulse–response model flux fraction (f_i) and lifetime (τ_i) parameters (see Figure 1 and Equations 1 and 2)

Pool name	f_i	τ_i (y)
CO_2_1	0.2763[b]	4.304[b]
CO_2_2	0.2824[b]	36.54[b]
CO_2_3	0.2240[b]	394.4[b]
CO_2_4	0.1473[c]	7000[c]
CO_2_5	0.0700[c]	200 000[c]
CH_4	1.0	12.4[d]

[a]Mean model from Joos et al. (2013).
[b]modified from Joos et al. (2013): CO_2_4 pool added; CO_2_5 pool flux fraction reduced from 0.2173 to 0.0700, and lifetime reduced from effectively infinite to 200,000 years (Archer et al., 1997, 1998).
[c]Myhre et al. (2013).

15 Earth System Models including full Earth System Models, Earth System Models of Intermediate Complexity (EMICs), and box-type models. However, these models were only run for up to 1,000 years, and so, their results lack information on multimillennial scale responses. The model modification used here includes an additional slow-response pool with a 7,000-year lifetime (CO_{2_4} in Figure 1 Table 3) in order to include ocean-sediment interactions (mainly calcium carbonate compensation) within the carbon cycle. The remaining long-term pool (CO_{2_5}) is given a lifetime of 200,000 years, related to a re-equilibration of the weathering-burial component of the carbon cycle (Archer, Kheshgi, & Maier-Reimer, 1997, 1998).

For methane, the atmospheric perturbation due to emission flux $\Phi_{CH4}(t)$ is given by

$$CH_4(t) = \int_0^t \Phi_{CH_4}(t')e^{(t'-t)/\tau_{CH_4}}\,dt' \tag{2}$$

For methane, we use a perturbation lifetime, τ_{CH4}, of 12.4 years (Myhre et al., 2013). We simulate the peatland atmospheric flux perturbations as annual net fluxes of CO_2 and CH_4 from peatland initiation through to 1,000 years after land-use conversion occurring in 2010 CE (see Tables 1 and 2). We approximate the integrals in Equations 1 and 2 with an annual time step discretization.

Peat accumulation rates are estimated for each site from the same radiocarbon-dated peat cores as in the GWP analysis, with the assumption of a constant rate of accumulation between profile dates (see Supporting Information Table S1 for values). Frolking and Roulet (2007) showed that variations around this constant flux assumption caused variations in the atmospheric burden perturbation, but had no significant impact on overall trends. Upon conversion, as a first approximation, we assume losses to persist until all peat is gone, at which time net CO_2 and CH_4 fluxes go to zero. We also assume that all aboveground vegetation C is released as CO_2 in the conversion year (instantaneous combustion, cf. IPCC 2014). For two tropical sites (Marudi and Lower Baram), we also test the atmospheric impact if emissions from land-use conversion stop after one or several 25-year oil palm rotations, after which the system either becomes CO_2 and CH_4 neutral (no net flux), or returns to predisturbance mean uptake rates (i.e., extremely rapid and effective restoration).

To explore the general behavior of the impulse-response model, we also consider four generalized zero-net C flux scenarios, with slow or fast CO_2 uptake followed by slow or fast CO_2 release. The slow rate was similar to the rate of CO_2 sequestration in peat (4 Mg CO_2 ha^{-1} $year^{-1}$ for 5,000 years (total = 20,000 Mg CO_2 ha^{-1} = 5,455 Mg C ha^{-1}). The fast rate was characteristic of drained tropical peatland CO_2 loss (66 Mg CO_2 ha^{-1} $year^{-1}$ for 303 years (total = 20,000 Mg CO_2 ha^{-1}). All four scenarios were run for 11,000 years, starting 5,000 years before the switch from CO_2 uptake to CO_2 release. The CO_2 flux was zero for the two fast-uptake scenarios until 303 years before the switch and was zero in all scenarios after all sequestered C had been released back to the atmosphere.

2.3.2 | Computing radiative forcing with the impulse-response model

Radiative forcing is an induced change in the Earth's energy budget and expressed in Watt [W] per square meter [m^2] of the Earth's surface (Forster et al., 2007). The global rate of radiative forcing (RF) perturbation due to net peatland CO_2 and CH_4 fluxes will be directly proportional to the atmospheric perturbation concentrations (Frolking, Roulet, & Fuglestvedt, 2006). For CH_4, the proportionality constant is a product of methane's radiative efficiency (3.63×10^{-4} W m^{-2} ppb^{-1} CH_4) and an indirect effects multiplier of 1.65 (Myhre et al., 2013), whereas for CO_2 the proportionality constant is only the CO_2 radiative efficiency (0.137×10^{-4} W m^{-2} ppb^{-1} CO_2). We convert between units of ppb to mass using 2.78 Tg CH_4 per ppb (Denman et al., 2007), and, by molar equivalence, 7.65 Tg CO_2 per ppb. We calculate the effect of 1 hectare [ha] of peatland on radiative forcing, hence results are expressed as W/m^2 per hectare.

The reference value for zero radiative forcing from a perturbation is arbitrary, but fixed to the system at a particular point in time. We consider two reference values. One sets zero at the time of peat initiation, that is, different for each site and varying from 1,500 to 8,000 years BP (Table 1), and $RF_{init}(t)$ is computed for all time after initiation. The other reference value follows the IPCC convention and is set to the end of the preindustrial period (i.e., 1750 CE; Myhre et al., 2013), and $RF_{1750}(t)$ is computed only after 1750 CE. By this time, most of the peat carbon that will be present at conversion has already been sequestered (Dommain et al., 2014), and the rest of the Earth system has been responding to the pre-1750 peat carbon sequestration (Equation 1). Due to methane's short atmospheric lifetime, for constant flux these two methods are essentially equivalent after 1800 CE. We evaluated the radiative forcing calculations by driving the impulse-response model with 100 kg pulse emissions of CO_2 and CH_4 and then integrating the resulting CO_2 and CH_4 radiative forcings for 20, 100, and 500 years, and computing their ratio,

$$GWP_T = \frac{\int_0^T RF_{CH_4}(t)dt}{\int_0^T RF_{CO_2}(t)dt} \tag{3}$$

which should equal published methane GWP values for T = 20, 100, or 500 years.

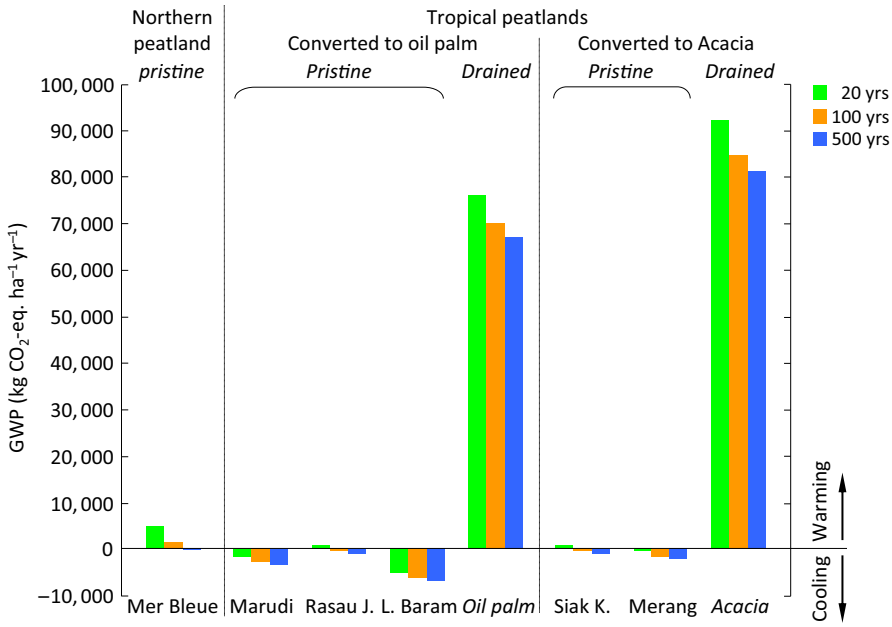

FIGURE 2 Global warming potentials (GWP) for the northern (undrained) Mer Bleue peatland and for five tropical peatlands under natural and drained, either oil palm or *Acacia* pulp plantation, conditions. GWPs are given for one hectare peatland and for 20-, 100-, and 500-year time horizons. Negative (positive) values denote CO_2-equivalent sinks (sources) and climatic cooling (warming)

3 | RESULTS

3.1 | Global Warming Potentials

The methane GWP test of the impulse-response model generated GWP_{20} = 85 kg CO_{2eq}/kg CH_4, and GWP_{100} = 28 kg CO_{2eq}/kg CH_4, values that are very similar to those reported by IPCC AR5 that exclude carbon cycle feedbacks (GWP_{20} = 84 and GWP_{100} = 28; table 8.7 in Myhre et al., 2013). We also used this model to compute a GWP_{500} value for methane of 8.2 kg CO_{2eq}/kg CH_4. This value is somewhat higher than the IPCC AR4 GWP_{500} value for methane of 7.6 kg CO_{2eq}/kg CH_4 (Forster et al., 2007), which was derived using a smaller indirect effects multiplier of 1.3.

In their prior pristine state the five tropical peatlands sequestered an estimated 1,063–7,036 kg CO_2 ha^{-1} $year^{-1}$ as a result of peat accumulation while releasing 22.5 kg CH_4 ha^{-1} $year^{-1}$ (Table 1). The corresponding GWPs at the 20-year time horizon for these carbon fluxes range from slightly positive (i.e., warming) to strongly negative (i.e., cooling) (Figure 2). The average net CO_{2eq} flux of all five sites in pristine condition is ca. −1,100 kg CO_{2eq} ha^{-1} $year^{-1}$ at the 20-year time horizon (Figure 2), whereas all tropical sites also have large negative net CO_{2eq} flux values for both the 100- and 500-year time horizons (Figure 2). In contrast, the temperate Mer Bleue peatland exhibits higher positive net CO_{2eq} flux (i.e., warming) for the 20- and 100-year time horizons and a comparatively low negative net CO_{2eq} flux for the 500-year time horizon (Figure 2), due to its comparatively lower average rate of CO_2 sequestration (750 kg CO_2 ha^{-1} $year^{-1}$) and higher average CH_4 emission rate (65 kg CH_4 ha^{-1} $year^{-1}$) (Table 1).

After their conversion to plantations, the oil palm sites released 66,000 kg CO_2 ha^{-1} $year^{-1}$, whereas *Acacia* sites release 80,000 kg CO_2 ha^{-1} $year^{-1}$. These conversions also led to an increase in CH_4 emissions to about 120 kg CH_4 ha^{-1} $year^{-1}$ (oil palm) and 140 kg CH_4 ha^{-1} $year^{-1}$ (*Acacia*) (Table 2) because of additional emissions from ditches, which have an average area cover of 3.7% in oil palm sites and 4.3% in *Acacia* plantations (Table 2, Supporting Information Figure S3). This overall shift in the greenhouse gas budget after drainage results in highly positive net CO_{2eq} fluxes (i.e., warming) for the 20-, 100-, and 500-year time horizons in the oil palm and *Acacia* plantation types. Postconversion greenhouse gas emissions and radiative forcing are strongly dominated by CO_2, minimizing the importance of the choice of time horizon for computing CO_{2eq} emissions (Figure 2).

3.2 | Perturbations of atmospheric CO_2 and CH_4 and radiative forcing

3.2.1 | Natural conditions (from peat initiation to 2010 CE)

The net sequestration of CO_2 by peat swamp forests generates a negative atmospheric CO_2 perturbation over several millennia (with most of the carbon stored in peat and only a lesser amount in aboveground biomass) (Figure 3a–c). In contrast, peatland CH_4 emissions produce a positive atmospheric perturbation for CH_4 (Figure 3a–c). However, this atmospheric methane perturbation is quite small relative to that of CO_2 (Figure 3c), because of the combined effects of a low flux rate and the short atmospheric lifetime of methane. The radiative forcing (RF_{init}) due to CO_2 and CH_4 are directly proportional to the magnitude and sign of their perturbations and are dominated by CO_2 (net cooling) effects. The exception to this behavior occurs during the initial 145 years of the temperate Mer Bleue simulation (Figure 3d, Table 4), as Mer Bleue initially had a relatively high CH_4 flux coupled with slower CO_2 uptake, which caused the initial net radiative forcing to be positive (warming).

At the time of its conversion in 2010 CE, the ~4900-year-old Marudi site in Borneo had accumulated ~5,450 Mg C ha^{-1} in peat and aboveground biomass (Figure 3a). This carbon pool corresponds

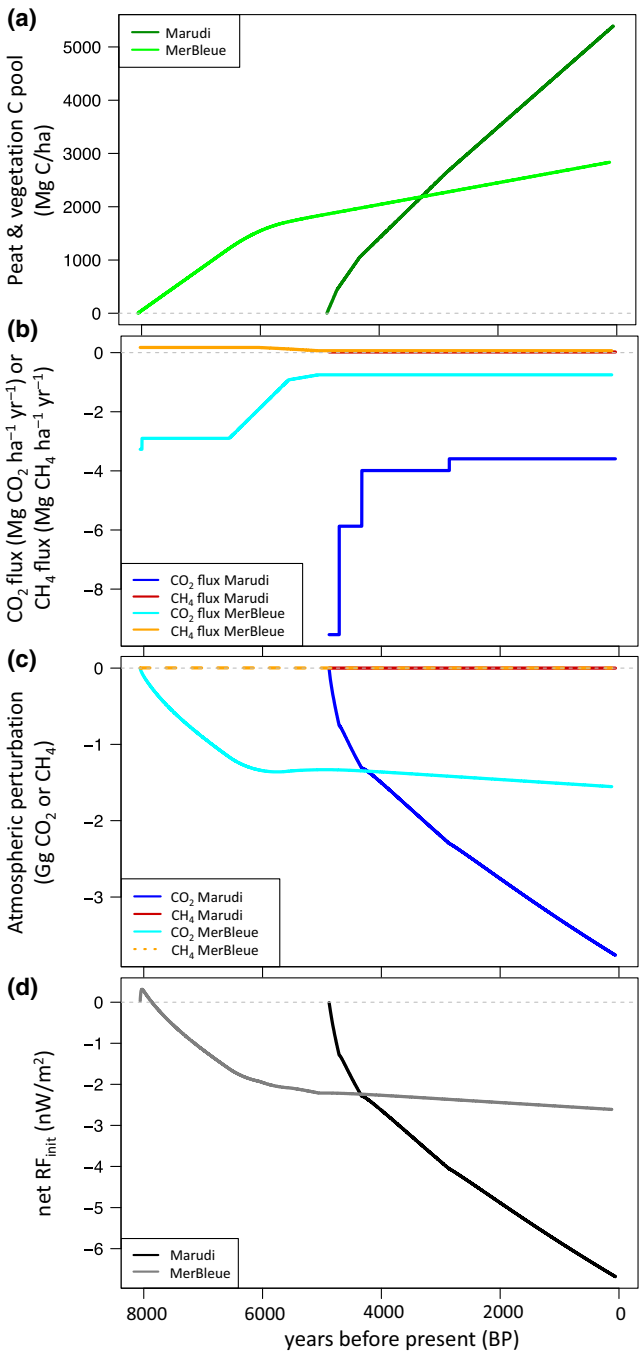

FIGURE 3 (a) Accumulating peat and vegetation C (Mg C ha^{-1}) for the Marudi and Mer Bleue sites. (b) Net CO_2 and CH_4 fluxes per hectare of peatland for the Marudi (tropical) and Mer Bleue (temperate) pristine sites (Mg CO_2 ha^{-1} $year^{-1}$ or Mg CH_4 ha^{-1} $year^{-1}$, sign convention is positive flux is to the atmosphere). CO_2 flux is consistent with peat plus vegetation C uptake in panel (a). (c) Atmospheric burden perturbation (Gg) for CO_2 (blue lines) and CH_4 (red lines) per hectare of peatland for the Marudi and Mer Bleue sites. (d) Net radiative forcing relative to peat initiation baseline (RF_{init}, nW/m^2) due to CO_2 and CH_4 perturbations (see panel c) per hectare of peatland for the Marudi and Mer Bleue sites; a positive RF is a net warming impact. Years before present: 0 BP = 1950 CE

to a cumulative net CO_2 flux of ca. −20,000 Mg CO_2 ha^{-1}. Considered in isolation, such a carbon uptake by peat is expected to lead to a net atmospheric perturbation of −3,810 Mg CO_2 (Table 4) or 1,040 Mg C. The cumulative CH_4 flux was +110 Mg CH_4 ha^{-1} by 2010 CE with a resulting expected atmospheric perturbation of +0.28 Mg CH_4. These atmospheric greenhouse gas perturbations would be equivalent to a net radiative forcing impact (RF_{init}) of about −6.7 nW/m^2 per hectare of peatland at Marudi in 2010 CE (Figures 3d and 4) relative to the mid-Holocene, 4,900 years ago. Relative to the preindustrial period (~1750 CE), the RF_{1750} in response to peat–carbon uptake at Marudi is small in 2010 CE, as only about 4% of the Marudi peat was sequestered after 1750 CE (see Figure 1a). The four other tropical peatland sites showed similar results, although all had accumulated less peat–carbon, and hence produced smaller atmospheric CO_2 perturbations and weaker RF_{init} cooling impacts by 2010 CE (Figure 4b, Table 4). Using 1750 CE as a baseline for radiative forcing, RF_{1750} values of the other four sites ranged from −0.15 to −1.0 nW/m^2 per hectare of peatland in 2010 CE.

In contrast, the temperate Mer Bleue peatland had a lower mean peat C accumulation rate than that of the tropical sites (Table 1), accumulating a carbon pool of 2,860 Mg C ha^{-1} by 2010 CE (Figure 2a). This value corresponds to a cumulative CO_2 flux of −10,480 Mg CO_2 ha^{-1} and an atmospheric perturbation of −1,575 Mg CO_2 (Table 4). Mer Bleue had moderate CH_4 fluxes, particularly in the first 2000 years after initiation (Figure 2a). After an initial one and a half-century of net positive RF_{init}, peaking at about +0.15 nW/m^2 per hectare of peatland, the cumulative impact of CO_2 uptake overwhelms the release of methane producing an increasingly negative radiative forcing that dominates its overall climatic impact for the rest of the Holocene. At present, the RF_{init} of Mer Bleue is about −2.7 nW/m^2 per hectare (Figure 3d) relative to the early Holocene. This cooling effect is similar to that of the youngest tropical site, the Lower Baram peatland (Figure 4b), which is only one-fifth as old as the Mer Bleue bog (Table 4). RF_{1750}, the contemporary radiative forcing relative to 1750 CE, is much smaller.

3.2.2 | Anthropogenically drained conditions (post-2010 CE)

Deforestation and drainage of peat swamp forests produce an immediate shift in net CO_2 exchange from net uptake to loss at about 15–30 times the uptake rate (Figure 4a; Tables 1 and 2). The rapid C loss caused by drainage produces an abrupt reversal in the trajectory of the modeled atmospheric CO_2 burden. Within several decades the atmospheric perturbation becomes positive and continues to rise until all the peat is consumed (Figure 4). This positive CO_2 perturbation peak is characteristic of all sites (Figure 4b).

Methane emissions also increase with land conversion, so the modeled methane atmospheric perturbation also increases to a larger value. The maximum of this increase is reached within several decades because of methane's short atmospheric lifetime. Despite

TABLE 4 Impulse-response model impact on atmosphere and radiative forcing relative to peat initiation baseline (RF_{init}), per hectare of peatland converted to *Acacia* or oil palm; sign convention is positive flux to atmosphere; atmospheric and radiative forcing perturbations are due to peat fluxes since initiation of peat accumulation. All values are per hectare of peatland converted and are rounded to two significant figures or the nearest year

Variable	Marudi	Rasau Jaya	Lower Baram	Siak Kanan	Merang	Mer Bleue
Initial RF_{init} switchover[a] (y)	1[b]	1[b]	1[b]	1[b]	1[b]	145
Cumulative CO_2 flux to 2010 (Mg CO_2 ha^{-1})	−20,000	−12,000	−4,600	−15,000	−4,900	−10,000
Cumulative CH_4 flux to 2010 (Mg CH_4 ha^{-1})	+110	+95	+35	+120	+39	+800
C in peat plus vegetation in 2010[c] (Mg C/ha)	5,500	3,300	1,300	4,000	1,300	2,900
Atmosphere CO_2 perturbation in 2010 (Mg CO_2) and as % of cumulative flux (in parentheses)	−3,800 (19%)	−2,200 (18%)	−1,300 (28%)	−2,700 (18%)	−1,200 (24%)	−1,600 (16%)
Atmosphere CH_4 perturbation in 2010 (Mg CH_4)	+0.28	+0.28	+0.28	+0.28	+0.28	+0.81
Atmosphere RF_{init} perturbation in 2010 (nW/m^2)	−6.7	−3.8	−2.4	−4.7	−2.1	−2.6
Years to postconversion shift to positive CO_2 and RF_{init} perturbation[d]	92	41	16	42	10	NA[f]
Years to peak of positive CO_2 and RF_{init} or RF_{1750} perturbation[e]	293	172	60	175	52	NA
Magnitude of positive CO_2 (RF_{init}) perturbation peak, Mg CO_2 (nW/m^2)	+4700 (+8.7)	+3400 (+6.4)	+1400 (+2.7)	+4100 (+7.8)	+1700 (+3.3)	NA
Magnitude of CO_2 (RF_{init}) perturbation in 2100 CE, Mg CO_2 (nW/m^2)	−190 (−0.03)	+1300 (+2.7)	+910 (+1.7)	+1500 (+3.1)	+1000 (+1.9)	NA
Magnitude of CO_2 (RF_{init}) perturbation in 2300 CE, Mg CO_2 (nW/m^2)	+4600 (+8.6)	+2100 (+3.8)	+430 (+0.77)	+2600 (+4.6)	+520 (+0.93)	NA
Magnitude of CO_2 (RF_{init}) perturbation in 3000 CE, Mg CO_2 (nW/m^2)	+1300 (+2.4)	+760 (+1.4)	+120 (+0.21)	+930 (+1.7)	+140 (+0.26)	NA

[a]Time after peat initiation at which net CO_2 plus CH_4 radiative forcing goes negative (Frolking et al., 2006).
[b]Site has negative net radiative forcing (CO_2 plus CH_4) immediately after initiation (i.e., at the end of simulation year 1, see Figure 2d).
[c]Also equals total C loss to atmosphere after land-use conversion in C mass units, and cumulative CO_2 flux (row 2).
[d]Time after land-use conversion in which net radiative forcing relative to peat initiation baseline (CO_2 plus CH_4) switches from negative to positive (see Figure 4); relative to preindustrial baseline, RF_{1750} is positive 1 year after conversion.
[e]Time after land-use conversion in which net radiative forcing (CO_2 plus CH_4) reaches maximum positive value (see Figure 4).
[f]Not applicable; land-use conversion has not happened at the Mer Bleue site.

methane's higher radiative efficiency per kg, and its indirect effects multiplier, the radiative impact of CH_4 is always <4% that of CO_2. Since the methane perturbation to the atmosphere continues to be small at all sites, the net radiative forcing continues to be approximately proportional to the CO_2 perturbation.

At the Marudi site, less than 300 years will be required after conversion to oxidize all the peat that accumulated over its nearly 4900 years of C sequestration (Figure 4a; Table 1). This loss causes the net global RF_{init} to rise from about −6.7 nW/m^2 (per hectare of converted peatland) through zero to about +8.7 nW/m^2 by the time all the peat is gone (Table 4). Under our assumption of no CO_2 flux after all the peat has been lost, the atmospheric CO_2 perturbation burden then relaxes back toward zero over the remainder of the simulation which takes several millennia (Figure 4a, Table 4). The other oil palm sites (Rasau Jaya and Lower Baram Delta) accumulated less peat by the time of their conversion (Table 1) and their warming impact on the atmosphere is smaller, reflected in the lower magnitude and shorter duration of their positive peaks (Figure 4b; Table 4). The C loss rate from the *Acacia* sites is about 20% higher than that from oil palm sites. This more rapid emission rate produces a positive peak in RF_{init} at the Siak Kanan site that is almost as large as that of the Marudi site, even though Siak Kanan had only 72% as much peat as Marudi at the time of conversion. Similarly, the peak radiative forcing of the Merang *Acacia* site is slightly larger than that of the Lower Baram oil palm site, despite their similar carbon pools at the time of conversion (Figure 4b; Table 4). For these latter sites with relatively shallow peat, the atmospheric CO_2 and positive RF_{init} perturbations drop close to zero by 3000 CE (Figure 4b).

Considering the 1750 CE reference point, for all sites RF_{1750} rose to positive radiative forcing the year of conversion (Figure 5) and continued to rise by the same amount as did RF_{init} (see Figure 4b), peaking at +4 nW/m^2 per hectare (Lower Baram Delta oil palm) to +14 nW/m^2 per hectare (Marudi oil palm), when all peat was gone. The RF_{1750} decay trajectories were closely parallel to the RF_{init}, and the RF_{1750} values had dropped to +1.2 to +7.7 nW/m^2 per hectare 1,000 years after conversion (Figure 5).

For scenarios in which peat oxidation at Marudi and Lower Baram stopped before all peat had been depleted, the rising CO_2

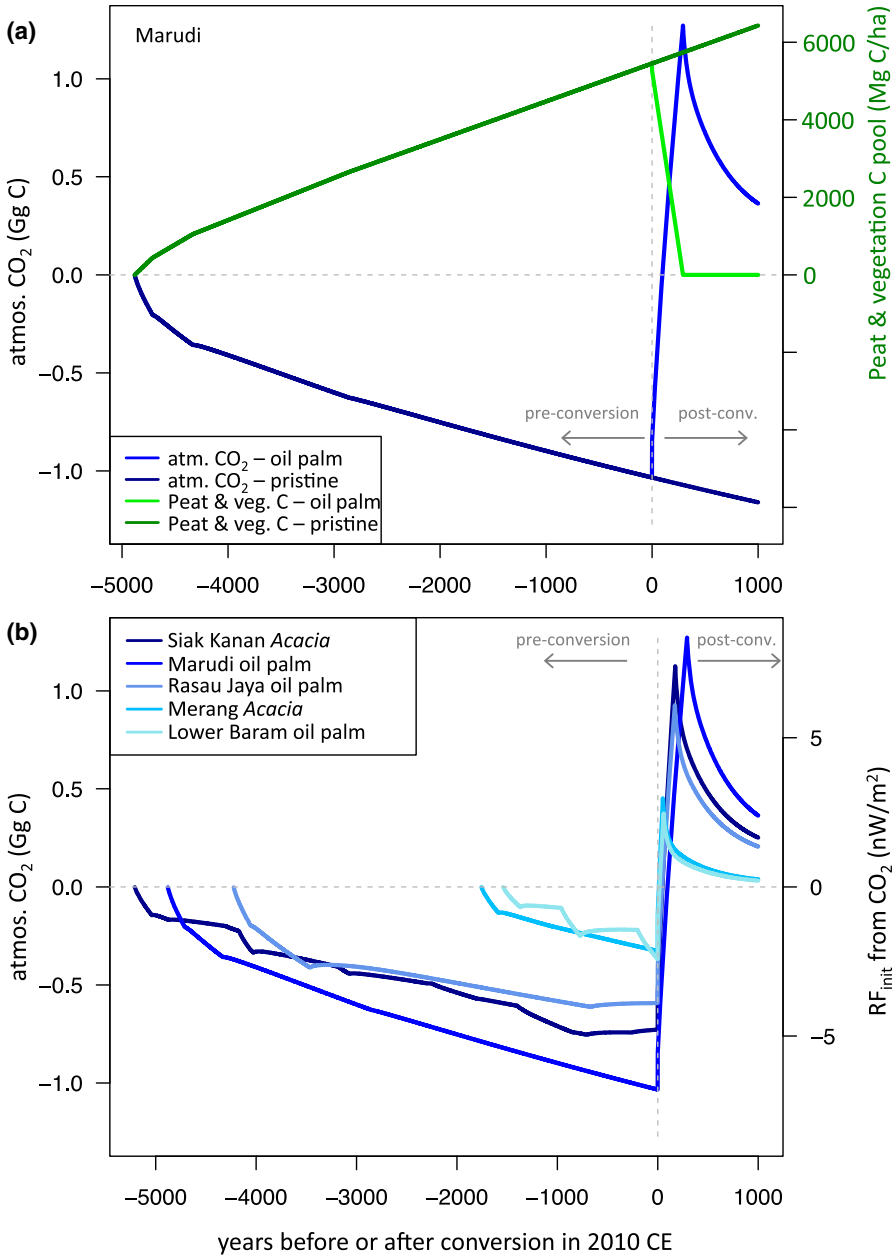

FIGURE 4 (a) Accumulating peat C (Mg C ha^{-1}) for Marudi with no land-use conversion (dark green line), and with conversion to oil palm in 2010 CE (light green line). Note that the land-use conversion scenario has no recovery or restoration (i.e., CO_2 flux equals zero) after all peat has been oxidized (light green line). Net atmospheric CO_2 burden perturbation (Gg C) per hectare of peatland for the Marudi pristine site with no conversion (dark blue line) and for conversion to oil palm in 2010 CE, after which there is a constant peat loss rate for 293 years until all peat is gone (lighter blue line). Vertical dashed line marks occurrence of land conversion to oil palm. Note that 6,000 Mg C = 6 Gg C. (b) Net atmospheric CO_2 burden perturbation (Gg C, left axis) and radiative forcing relative to peat initiation baseline due to CO_2 (RF_{init}, nW/m^2, right axis) per hectare of peatland for five tropical peatland land-use scenarios, all converted to oil palm or *Acacia* in 2010 CE (see Table 1); in all cases, simulations assume that CO_2 flux goes to zero once all peat is lost. The kinks in the atmospheric CO_2 burden prior to land-use conversion for some of the sites arise from the significant changes in peat C accumulation rates during the preceding millennia (see Supporting Information Table S1—peat core CO_2 uptake data). Note: the horizontal axis is time; land-use conversion is in 2010 CE for all cases considered (Table 1), so −60 years = 1950 CE = 0 BP; for example, −2060 years is 2000 BP, and +250 years is 2260 CE

perturbation also ceased when the loss of peat stopped. Then it relaxed back to an equilibrium value associated with the total amount of C still remaining in the peat under the assumption of zero flux after the interval of peat loss ended (Supporting Information S.3 and Figure S4).

3.2.3 | Generalized Radiative Forcing Scenarios

Of the four hypothetical, generalized scenarios, the positive peak in the atmospheric CO_2 perturbation and radiative forcing following the shift from ecosystem CO_2 uptake to loss was earliest and largest

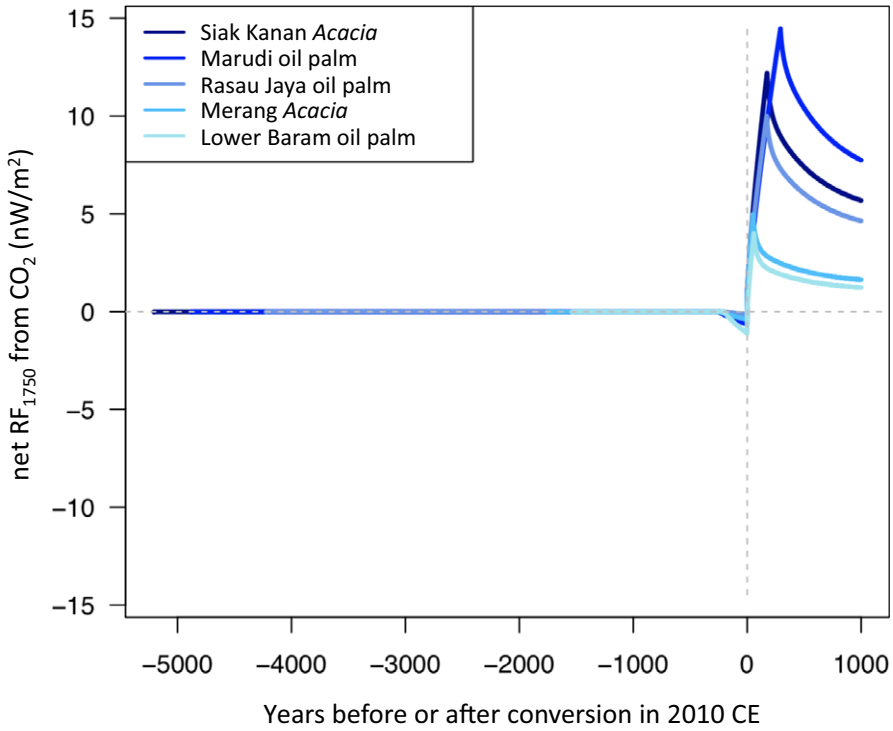

FIGURE 5 Net radiative forcing relative to preindustrial baseline due to CO_2 (RF_{1750}, nW/m^2) per hectare of peatland for five tropical peatland land-use scenarios, all converted to oil palm or *Acacia* in 2010 CE (see Table 1); in all cases, simulations assume that CO_2 flux goes to zero once all peat is lost. Note: the horizontal axis is time; land-use conversion is in 2010 CE for all cases, so −60 years = 1950 CE = 0 BP; for example, −2060 years is 2000 BP, and +250 years is 2260 CE

for the slow-uptake/fast-release scenario (Figure 6). Slower CO_2 release not only delays but also diminishes the magnitude of the shift from a net cooling to warming impact on the Earth's radiation budget (Figure 6; see Supplemental Figure S6 for the behavior of the individual CO_2 pools in these generalized scenarios). Fast CO_2 uptake increases the magnitude of the negative atmospheric perturbation by a factor of two at the time of conversion relative to slow-uptake, but the peak of the positive CO_2 shift for the fast-uptake/fast-release scenario is only half as high as that of the slow-uptake/fast-release scenario (Figure 6).

4 | DISCUSSION

Two different methods were used to assess the climate impact of converting pristine tropical peatlands to agricultural plantations: the commonly applied global warming potential and an impulse-response model. Global warming potentials (GWP) provide a means to assess the climate impact of a pulse flux (here from a single year) of multiple greenhouse gases into a common metric. The result is a net equivalent CO_2 flux which can be expressed as a net emission (warming) or a net uptake (cooling). If methane flux is a significant factor, then the GWP values will be strongly dependent on the time horizon selected during the development of a peatland (Whiting & Chanton, 2001). GWP calculations are straightforward, but have several disadvantages: (a) they do not compute direct climate impacts, (b) they do not consider the continuous and varying fluxes of CO_2 and CH_4 over time that are characteristic of peatlands, and (c) they are not able to quantify the transient nature of the atmospheric impact of peatland carbon fluxes (Bridgham et al., 2014; Frolking & Roulet, 2007; Frolking et al., 2006; Neubauer, 2014; Neubauer & Megonigal, 2015).

In contrast, the impulse-response model computes a radiative forcing time series in units of W/m^2 in relation to constant, episodic, or temporally varying fluxes of multiple greenhouse gases. It considers these fluxes to cause perturbations to an otherwise constant atmosphere, and tracks the atmospheric recovery from these perturbations due to the rest of the Earth system (e.g., Frolking & Roulet, 2007; Joos et al., 1996, 2013; Neubauer & Megonigal, 2015). The results from the GWP and RF models are not directly comparable, as they estimate different quantities.

4.1 | Potential caveats and model evaluation

The simulations presented here have used multimillennial time series for variations in natural carbon storage (reconstructed from peat cores), but constant values for CH_4 and anthropogenic CO_2 fluxes (see Supporting Information Section S4.1). N_2O emissions have been omitted due to existing uncertainties in greenhouse gas emissions from tropical peatlands (but see Supporting Information Section S4.2). While fluxes for CH_4 and CO_2 should vary over time, the use of an average CH_4 flux and robust literature-based CO_2 emission values appears consistent for a first-order behavior analysis which focuses on general model responses. We have not included peat fire emissions in our conversion scenarios, as we assume that well-managed plantations are not likely to burn often. However, intense fires can occur in plantation areas during prolonged droughts (Gaveau et al., 2014). Peat fires would accelerate carbon losses, but these disturbances would not generally alter our results or conclusions

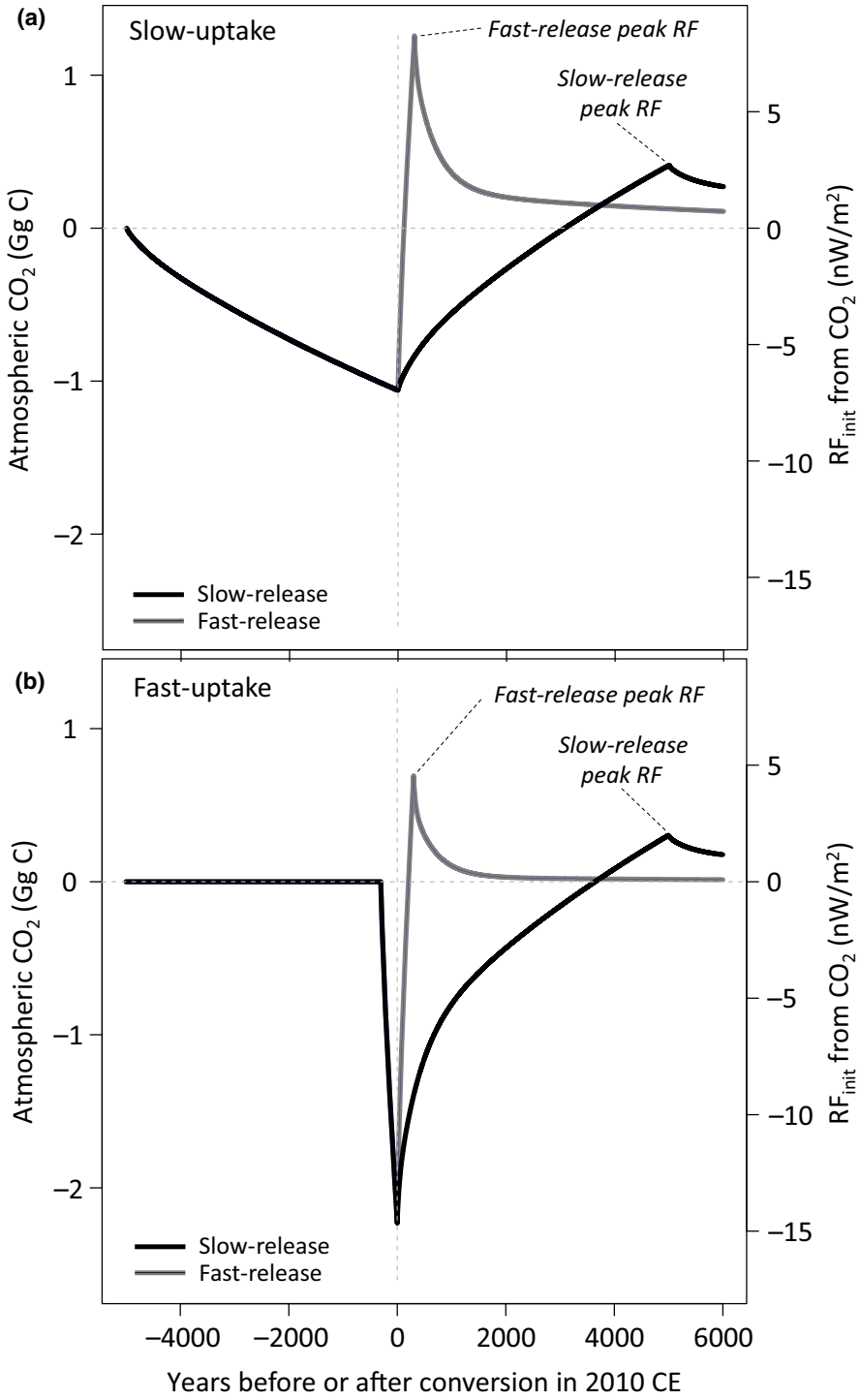

FIGURE 6 Four hypothetical net-zero fast/slow-uptake/release scenarios. (a) Net atmospheric CO_2 burden perturbation (Gg C, black line) per hectare of peatland for a hypothetical site with slow CO_2 uptake (400 g CO_2 m^{-2} year^{-1} for 5,000 years) followed by conversion in 2010 CE, and slow loss (black line) of that peat C to the atmosphere as CO_2 at the same rate (400 g CO_2 m^{-2} year^{-1} for 5,000 years) or fast loss (6,600 g CO_2 m^{-2} year^{-1} for 303 years, gray line). (b) Same as panel (a) but for rapid peat uptake (6,600 g CO_2 m^{-2} year^{-1} for 303 years). All simulations are started 5,000 years before "conversion" and continue for an additional 6,000 years

(Supporting Information Section S4.3). Long-term plantation land-use impacts are also uncertain, as most plantations in the region are less than a few decades old (Dommain et al., 2016; Miettinen et al., 2016). We discuss and analyze alternative conversion flux scenarios in Supplemental Section S3.

The simple atmospheric impulse-response model applied here neglects any nonlinearities in the carbon cycle, such as those associated with the carbonate chemistry in the ocean, with the dependency of terrestrial primary productivity on environmental conditions, or with climate–carbon cycle interactions (see Supporting Information Section S4.4). Our atmospheric RF model should be considered only an approximation (cf. Joos et al., 2013). We performed a set of idealized simulations with the Bern3D-LPX coupled Earth System Model of Intermediate Complexity (Ritz, Stocker, & Joos, 2011; Stocker et al., 2013) to evaluate the linear empirical representation of Earth system carbon cycling (Equation 1) in our impulse-response model, as well as its response to atmospheric gas flux perturbations for restricted model settings. We ran three CO_2

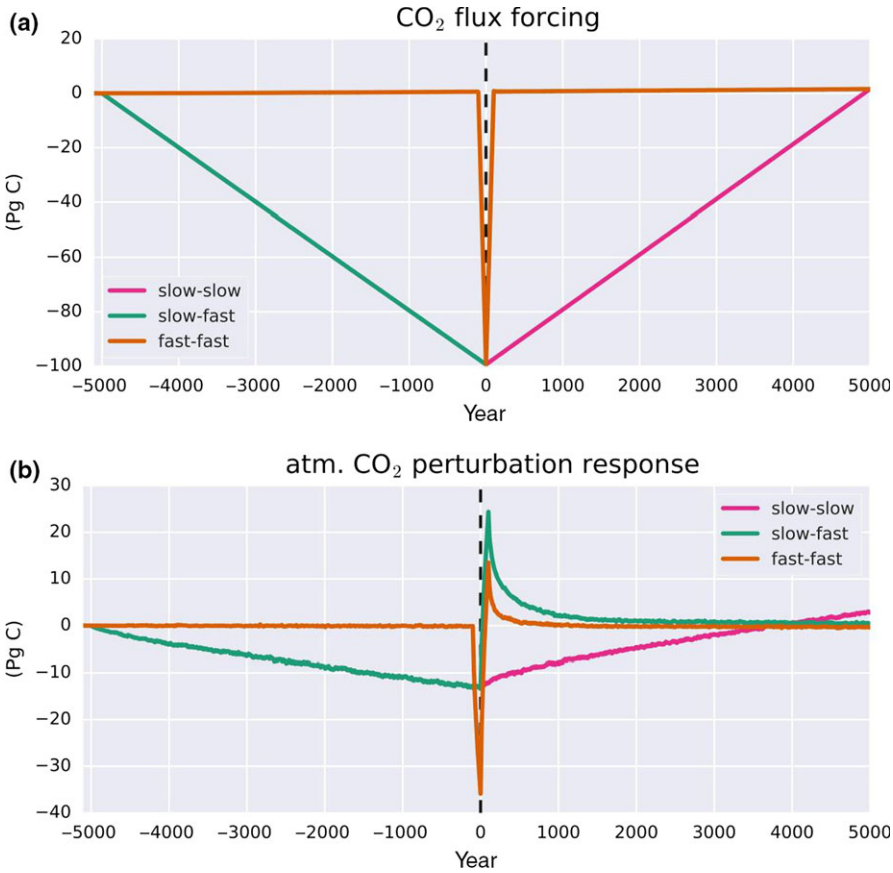

FIGURE 7 (a) Cumulative perturbation forcing CO_2 added to the atmospheric pool of the Bern3D-LPX model (see model description in supplement). Slow removal (pink line under green line) is at 0.02 Pg C/year for 5,000 years (total of 100 Pg C); fast removal (orange line) is at 1.0 Pg C/y for 100 years (total of 100 Pg C). Slow addition (pink line) is at 0.02 Pg C/years for 5,000 years (total of 100 Pg C); fast removal (green line under orange line) is at 1.0 Pg C/years for 100 years (total of 100 Pg C). (b) Bern3D-LPX simulated atmospheric CO_2 perturbation response to the three forcing scenarios of panel (a). t = 0 is simulation time of switch from CO_2 removal forcing to CO_2 addition forcing. Note that the y-axis scale differs between the panels

forcing scenarios for 10,000 years in which the atmosphere was perturbed with 100 Pg C, as in Joos et al. (2013), at slow- and/or fast-uptake and release rates (1 Pg C/year for 100 years or 0.02 Pg C/year for 5,000 years, Figure 7a, Supporting Information Section S.5), similar to the hypothetical net-zero scenarios presented above (Supporting Information Section 3.2.3.; Figure 6). The temporal patterns of atmospheric CO_2 perturbation due to these forcings (Figure 7) had very similar dynamics to the empirical fast/slow simulations (Figure 6) and thus support the general validity of the results of our impulse-response model scenarios.

Further, from the Bern3D-LPX model experiments, it is possible to set our impulse-response model into an Earth system context. Over the millennia of peat build-up, the negative atmospheric perturbation is balanced mainly by the ocean and ocean-sediment interactions (through calcium carbonate compensation), and changes in land vegetation which both lose carbon, leaving only a small atmospheric perturbation of about 12 Pg C at the time of conversion. Conversion of peatlands leads to a rapid release to the atmosphere of the carbon stored over millennia. Since the ocean and land biosphere cannot respond as rapidly, this leads to a positive CO_2 perturbation in the atmosphere (Figure 7b). Over time this positive perturbation is removed from the atmosphere as the ocean has time to equilibrate (Figure 7b and Supporting Information Figure S7a). In general, the nature of the atmospheric perturbation is a function of the rates and duration of CO_2 uptake and release, as these determine the magnitude of responses in other carbon pools of the Earth system. Over long timescales (millennia) responses of the ocean and ocean sediments play an important role.

4.2 | Global Warming Potentials of natural and drained tropical peatlands

The GWP analysis of contemporary pristine peatlands yields a stronger cooling (or weaker warming) effect for the tropical sites than for the northern Mer Bleue bog, because the tropical sites are characterized by lower CH_4 emissions and higher rates of CO_2 sequestration. With a molar CH_4:CO_2 exchange ratio of about 0.03 (Table 1), tropical peatlands are net greenhouse gas sinks, following the wetland GWP classification analysis of Whiting and Chanton (2001). This GWP perspective highlights the global climatic cooling effect of net carbon fluxes from the undisturbed peatlands in South-East Asia prior to their conversion to agricultural plantations.

Moreover, the GWP analysis indicates that the conversion and drainage of tropical peat swamp forests produce a dramatic shift from a net cooling to very strong warming impact, regardless of the time horizon (Figure 2). These results provide a strong contrast to chamber-flux-based findings of previous studies (e.g., Furukawa, Inubushi, Ali, Itang, & Tsuruta, 2005; Inubushi & Hadi, 2007; Melling et al., 2005a,b). This discrepancy arises because of a fundamental difference in the process measured. Our GWP analyses are based on rates of carbon sequestration calculated from radiocarbon-dated peat cores, which represent total ecosystem CO_2 uptake once vegetation

biomass has stabilized. Chamber-based flux measurements assess total peat surface CO_2 fluxes and are an incomplete measure of the total net ecosystem C flux.

Radiocarbon-dated peat cores provide the most robust estimates of the carbon balance of peat swamp forests over long timescales from the time of their inception to the present. In contrast, it is not possible to derive net carbon sequestration using chamber-based CO_2 flux measurements in forested ecosystems. Many chamber-based studies of South-East Asian peatlands have measured the combined short-term CO_2 flux from both heterotrophic soil and autotrophic root respiration, which is not representative of the total net peat carbon balance (Couwenberg et al., 2010). Unsurprisingly, these studies found higher total CO_2 fluxes from the floor of peat swamp forests than from oil palm plantations (e.g., Melling et al., 2005a; Melling et al. 2012), most likely due to the substantial contribution of autotrophic respiration from tree roots. As a result, they derived GWP values that are not representative of the long-term carbon balance. Based on the apparently higher GWP values of natural peatlands, they mistakenly concluded that peat swamp forests had a more detrimental impact on climate than oil palm plantations – a scientifically incorrect claim (Wijedasa et al., 2017). Our GWP and radiative forcing analyses clearly indicate that the conversion of tropical peatlands to oil palm or *Acacia* plantations creates significant "hot-spots" for CO_2 emissions to the atmosphere.

4.3 | Radiative forcing impact of pristine and converted tropical peatlands

Our analysis indicates that the long-term carbon accumulation in undisturbed tropical peatlands led, in isolation (i.e., RF_{init}), to an increasingly negative perturbation to atmospheric CO_2, and thus to an increasingly negative radiative forcing (cooling) relative to the mid to late Holocene. Yet, as CO_2 uptake persisted for centuries to millennia, this negative atmospheric perturbation would be partially offset by response of other carbon reservoirs in the Earth system (Figure 1). The modeled atmospheric perturbation (i.e., the net atmospheric reduction in CO_2) at the time of conversion (2010 CE) was 16-to-28% of the total CO_2 sequestered in the peat (Table 4). This percentage was lower for older peatlands, because of the gradual trend toward equilibration in the slow-response pool (CO_{2_4}) with a 7,000-year lifetime (Supporting Information Figures S4 and S5). The radiative forcing in 2010 CE ranged from −2.1 to −6.1 nW/m^2 per hectare of peatland (Table 4). For northern peatlands in aggregate, Frolking and Roulet (2007) computed a contemporary radiative forcing of about −0.4 W/m^2. Using a northern peatland area of 350 million ha (Frolking et al., 2011) we calculate a contemporary radiative forcing value for northern peatlands of about −1.2 nW/m^2 per hectare of peatland. This value is lower than that for tropical peatlands because of their lower mean density of peat carbon per hectare and higher mean methane emission rate. As with the GWP analysis, low methane emissions from tropical peatlands have a very small effect on the radiative forcing.

The drainage and conversion of tropical peat swamp forests to oil palm or *Acacia* plantations, including persistent lowering of the water table, leads to an immediate shift from a weak CO_2 sink to a strong CO_2 source (Figure 4; Couwenberg et al., 2010) that could potentially persist for many decades to a few centuries. This change in the direction of the CO_2 flux causes the trajectory of the atmospheric CO_2 perturbation to abruptly shift and leads to an immediate increase in atmospheric CO_2, and a positive radiative forcing, relative to preconversion and to a preindustrial 1750 CE reference (RF_{1750}). Considering the peatland in isolation (RF_{init}), it takes one to several decades to completely offset the existing negative perturbation that resulted from Holocene peat accumulation, and the perturbation peaks at the time CO_2 emissions stop (Figure 4, Supporting Information Figure S4, Table 4). Once all peat is oxidized, and net CO_2 flux goes to zero, the total atmospheric CO_2 burden, and RF_{init}, relax back toward zero, as there is no carbon remaining in the peat, and it all is gradually redistributed in the Earth system. However, this relaxation will take many centuries to millennia, because of the slow rate at which other Earth system components reset the carbon cycle to a new equilibrium state (Figures 4–6), due to long lifetimes associated with the ocean carbon cycle and calcium carbonate compensation (Supporting Information Figures S5, S6, and S8). The slow capacity of the Earth system to fully respond to the rapid rate of carbon loss from drained peatlands is primarily responsible for the positive atmospheric CO_2 perturbation and radiative forcing impact (RF_{init}) while there is still peat–carbon remaining (Figure 4, Supporting Information sections S.4 and S.5). These significant results emphasize the persistent long-term impact of just decades of oil palm and *Acacia* cultivation on drained peatlands on the global climate system. Quantifying the full extent of this climatic warming impact by considering all drained peatland area should be a high research priority.

4.4 | Climate significance of tropical peatlands

This study compares the long-term trajectory of climatic impacts produced by the carbon fluxes from tropical peatlands under both natural conditions and their recent conversion to agricultural plantations. The tropical peatlands of South-East Asia largely formed during the past 5,000 years and have persistently removed carbon dioxide from the atmosphere while releasing methane at a low rate. GWP analysis indicates that, while they remain pristine, tropical peatland sites are generally net equivalent sinks for CO_2, particularly over long time horizons. The impulse-response model also shows that in an undisturbed state, tropical peat swamp forests produce a negative radiative forcing effect (a net climatic cooling) from the time of their initiation that increases as they accumulate peat over time. Per unit area, tropical peatlands generally have a stronger negative radiative forcing effect than northern peatlands, highlighting the global climatic significance of these ecosystems.

The conversion of tropical peatlands to plantations drives a rapid destabilization of their carbon stocks that required several millennia to accumulate. This abrupt shift from a slowly accumulating carbon sink to a rapidly emitting source of CO_2 produces a strong positive

(warming) radiative forcing effect that is similar to or may slightly exceed the magnitude of the prior cumulative cooling. From the perspective of a preindustrial (1750 CE) baseline, tropical peatland conversion leads to an immediate and rapidly rising positive CO_2 and radiative forcing perturbation of the atmosphere. Moreover, this net warming impact will persist for centuries to millennia after all peat has been lost because of the long "effective-half-life" of CO_2 in the atmosphere. This strong shift in radiative forcing results from a rate of CO_2 release, which can persist for decades at 15-30 times the long-term CO_2 uptake rate of pristine peat swamp forests, a seemingly unique response among terrestrial ecosystems. This strong nonlinear forcing impact on the atmosphere has not been previously documented for peatlands and provides a convincing argument against any further peatland conversion or continuation of drained plantation agriculture in the context of mitigating global climate change. Undisturbed tropical peatlands should be protected to preserve their significant climate regulation service, which would naturally continue to operate for many millennia—the natural lifetime of these peatlands (Cobb et al., 2017).

ACKNOWLEDGEMENTS

R.D. acknowledges financial support by Geo.X, the Research Network for Geosciences in Berlin, and Potsdam. S.F. acknowledges financial support from NASA grant NNX14AD31G and USDA grant 10JV11242306135. F.J. and A.J. acknowledge support by the Swiss National Science Foundation (# 200020_172476). J.C. acknowledges financial support from the European Social Fund (ESF) and the Ministry of Education, Science and Culture of Mecklenburg-Western Pomerania (project WETSCAPES, ESF/14-BM-A55-0030/16).

ORCID

René Dommain http://orcid.org/0000-0003-4547-8983

REFERENCES

Archer, D., Kheshgi, H., & Maier-Reimer, E. (1997). Multiple timescales for neutralization of fossil fuel CO_2. *Geophysical Research Letters*, *24*, 405–408. https://doi.org/10.1029/97GL00168

Archer, D., Kheshgi, H., & Maier-Reimer, E. (1998). Dynamics of fossil fuel CO_2 neutralization by marine $CaCO_3$. *Global Biogeochemical Cycles*, *12*, 259–276. https://doi.org/10.1029/98GB00744

Bonan, G. B. (2008). Forests and climate change: forcings, feedbacks, and the climate benefits of forests. *Science*, *320*, 1444–1449. https://doi.org/10.1126/science.1155121

Bridgham, S. D., Moore, T. R., Richardson, C. J., & Roulet, N. T. (2014). Errors in greenhouse forcing and soil carbon sequestration estimates in freshwater wetlands: a comment on Mitsch et al. (2013). *Landscape Ecology*, *29*, 1481–1485. https://doi.org/10.1007/s10980-014-0067-2

Carlson, K. M., Goodman, L. K., & May-Tobin, C. C. (2015). Modeling relationships between water table depth and peat soil carbon loss in Southeast Asian plantations. *Environmental Research Letters*, *10*, 074006. https://doi.org/10.1088/1748-9326/10/7/074006

Cobb, A. R., Hoyt, A. M., Gandois, L., Eri, J., Dommain, R., Salim, K. A., … Harvey, C. F. (2017). How temporal patterns in rainfall determine the geomorphology and carbon fluxes of tropical peatlands. *Proceedings of the National Academy of Sciences*, *114*, E5187–E5196.

Couwenberg, J., Dommain, R., & Joosten, H. (2010). Greenhouse gas fluxes from tropical peatlands in Southeast Asia. *Global Change Biology*, *16*, 1715–1732.

Couwenberg, J., & Hooijer, A. (2013). Towards robust subsidence-based soil carbon emission factors for peat soils in south-east Asia, with special reference to oil palm plantations. *Mires & Peat*, *12*, 1–13.

Denman, K. L., Brasseur, G., Chidthaisong, A., Ciais, P., Cox, P. M., Dickinson, R. E., … Zhang, X. (2007). Couplings between Changes in the Climate System and Biogeochemistry. In S. Solomon, D. Qin, M. Manning, Z. Chen, M. Marquis, K. B. Averyt, M. Tignor & H. L. Miller (Eds.) *Climate Change 2007: the Physical Science Basis. Contribution of Working Group I to the Fourth Assessment Report of the Intergovernmental Panel on Climate Change* (pp. 499–587). Cambridge, UK and New York, NY: Cambridge University Press.

Dommain, R., Couwenberg, J., Glaser, P. H., Joosten, H., & Suryadiputra, I. N. N. (2014). Carbon storage and release in Indonesian peatlands since the last deglaciation. *Quaternary Science Reviews*, *97*, 1–32. https://doi.org/10.1016/j.quascirev.2014.05.002

Dommain, R., Couwenberg, J., & Joosten, H. (2011). Development and carbon sequestration of tropical peat domes in south-east Asia: Links to post-glacial sea-level changes and Holocene climate variability. *Quaternary Science Reviews*, *30*, 999–1010. https://doi.org/10.1016/j.quascirev.2011.01.018

Dommain, R., Dittrich, I., Giesen, W., Joosten, H., Rais, D. S., Silvius, M., & Wibisono, I. T. C. (2016). Ecosystem services, degradation and restoration of peat swamps in the Southeast Asian tropics. In A. Bonn, T. Allott, M. Evans, H. Joosten, & R. Stoneman (Eds.), *Peatland Restoration and Ecosystem Services: Science, Policy and Practice* (pp. 253–288). Cambridge, UK: Cambridge University Press.

Drösler, M., Verchot, L. V., Freibauer, A., Pan, G., Evans, C. D., Borbonniere, R. A., … Wang, C. (2014). Chapter 2 Drained inland organic soils. In T. Hiraishi, T. Krug, K. Tanabe, N. Srivastava, J. Baasansuren, M. Fukuda & T. G. Troxler (Eds.) *2013 Supplement to the 2006 IPCC Guidelines for National Greenhouse Gas Inventories: Wetlands* (pp. 2.1–2.79). Switzerland: Intergovernmental Panel on Climate Change (IPCC).

Field, C. B., Lobell, D. B., Peters, H. A., & Chiariello, N. R. (2007). Feedbacks of terrestrial ecosystems to climate change. *Annual Review of Environment and Resources*, *32*, 1–29. https://doi.org/10.1146/annurev.energy.32.053006.141119

Foley, J. A., Costa, M. H., Delire, C., Ramankutty, N., & Snyder, P. (2003). Green surprise? How terrestrial ecosystems could affect earth's climate. *Frontiers in Ecology and the Environment*, *1*, 38–44.

Forster, P., Ramaswamy, V., Artaxo, P., Berntsen, T., Betts, R., Fahey, D. W., … Van Dorland, R. (2007). Changes in Atmospheric Constituents and in Radiative Forcing. In S. Solomon, D. Qin, M. Manning, Z. Chen, M. Marquis, K. B. Averyt, M. Tignor & H. L. Miller (Eds.) *Climate Change 2007: The Physical Science Basis. Contribution of Working Group I to the Fourth Assessment Report of the Intergovernmental Panel on Climate Change* (pp. 129–234). Cambridge, UK and New York, NY: Cambridge University Press.

Friborg, T., Soegaard, H., Christensen, T. R., Lloyd, C. R., & Panikov, N. (2003). Siberian wetlands: Where a sink is a source. *Geophysical Research Letters*, *30*, 2129–2132. https://doi.org/10.1029/2003GL017797

Frolking, S., & Roulet, N. T. (2007). Holocene radiative forcing impact of northern peatland carbon accumulation and methane emissions. *Global Change Biology*, *13*, 1079–1088. https://doi.org/10.1111/j.1365-2486.2007.01339.x

Frolking, S., Roulet, N., & Fuglestvedt, J. (2006). The impact of a northern peatland on the earth's radiative budget: Sustained methane emission versus sustained carbon sequestration. *Journal of Geophysical Research*, *111*, G01008.

Frolking, S., Roulet, N. T., Tuittila, E. S., Bubier, J. L., Quillet, A., Talbot, J., & Richard, P. J. H. (2010). A new model of Holocene peatland net primary production, decomposition, water balance, and peat accumulation. *Earth System Dynamics*, *1*, 1–21. https://doi.org/10.5194/esd-1-1-2010

Frolking, S., Talbot, J., Jones, M., Treat, C. C., Kauffman, J. B., Tuittila, E. S., & Roulet, N. T. (2011). Peatlands in the Earth's 21st century climate system. *Environmental Reviews*, *19*, 371–396. https://doi.org/10.1139/a11-014

Furukawa, Y., Inubushi, K., Ali, M., Itang, A. M., & Tsuruta, H. (2005). Effect of changing groundwater levels caused by land-use changes on greenhouse gas fluxes from tropical peat lands. *Nutrient Cycling in Agroecosystems*, *71*, 81–91. https://doi.org/10.1007/s10705-004-5286-5

Gaveau, D. L., Salim, M. A., Hergoualc'h, K., Locatelli, B., Sloan, S., Wooster, M., … Verchot, L. (2014). Major atmospheric emissions from peat fires in Southeast Asia during non-drought years: Evidence from the 2013 Sumatran fires. *Scientific Reports*, *4*, 6112.

Glaser, P. H., & Chanton, J. P. (2009). Methane accumulation and release from deep peat: Measurements, conceptual models, and biogeochemical significance. In A. J. Baird, L. R. B. Belyea, X. Comas, A. S. Reeve, & L. D. Slater (Eds.), *Carbon Cycling in Northern Peatlands, Geophysical Monograph Series 184* (pp. 145–158). Washington, DC: American Geophysical Union.

Gorham, E. (1991). Northern peatlands: Role in the carbon cycle and probable responses to climatic warming. *Ecological Applications*, *1*, 182–195. https://doi.org/10.2307/1941811

Hatano, R., Inoue, T., Yamada, H., Sato, S., Darung, U., Limin, S., … Bathgate, J. (2011). Soil greenhouse gases emissions from various land uses in tropical peatlands in Indonesia. In Suwardi, R. Hatano, B. Sumawinata, Darmawan, S. Limin & Y. A. Nion (Eds.) *Proceedings of Palangkaraya International Symposium and Workshop on Tropical Peatland Management. Palangkaraya, Indonesia, 10–11 June 2010 "The Proper Use of Tropical Peatland"* (pp. 47–55). Bogor, Indonesia: Integrated Field Environmental Science - Global Center of Excellence (IFES-GCOE) Indonesian Liaison Office.

Hooijer, A., Page, S., Canadell, J. G., Silvius, M., Kwadijk, J., Wösten, H., & Jauhiainen, J. (2010). Current and future CO_2 emissions from drained peatlands in Southeast Asia. *Biogeosciences*, *7*, 1505–1514. https://doi.org/10.5194/bg-7-1505-2010

Hooijer, A., Page, S., Jauhiainen, J., Lee, W. A., Lu, X. X., Idris, A., & Anshari, G. (2012). Subsidence and carbon loss in drained tropical peatlands. *Biogeosciences*, *9*, 1053–1071. https://doi.org/10.5194/bg-9-1053-2012

Inubushi, K., & Hadi, A. (2007). Effect of land-use management on greenhouse gas emissions from tropical peatlands. In J. O. Rieley, C. J. Banks & B. Radjagukguk (Eds.) *Carbon–Climate–Human Interaction on Tropical Peatland. Proceedings of the International Symposium and Workshop on Tropical Peatland, Yogyakarta* (p. 29). Leicester, UK: CARBOPEAT, Department of Geography, University of Leicester.

IPCC (2013). Climate Change 2013: The Physical Science Basis. In T. F. Stocker, D. Qin, G.-K. Plattner, M. Tignor, S. K. Allen, J. Boschung, A. Nauels, Y. Xia, V. Bex & P. M. Midgley (eds.). *Contribution of Working Group I to the Fifth Assessment Report of the Intergovernmental Panel on Climate Change* (pp. 1535). Cambridge, New York: Cambridge University Press.

Jauhiainen, J., Hooijer, A., & Page, S. E. (2012a). Carbon dioxide emissions from an Acacia plantation on peatland in Sumatra, Indonesia. *Biogeosciences*, *9*, 617–630. https://doi.org/10.5194/bg-9-617-2012

Jauhiainen, J., Hooijer, A., & Page, S. E. (2012b). Greenhouse gas emissions from a plantation on thick tropical peat. Extended abstract No. 220. In *Peatlands in Balance Proceeding of the 14th International Peat Congress, Stockholm, Sweden*.

Jauhiainen, J., & Silvennoinen, H. (2012). Diffusion GHG fluxes at tropical peatland drainage canal water surfaces. *Suo*, *63*, 93–105.

Joos, F., Bruno, M., Fink, R., Siegenthaler, U., Stocker, T. F., le Quéré, C., & Sarmiento, J. L. (1996). An efficient and accurate representation of complex oceanic and biospheric models of anthropogenic carbon uptake. *Tellus*, *48*, 397–417. https://doi.org/10.1034/j.1600-0889.1996.t01-2-00006.x

Joos, F., Roth, R., Fuglestvedt, J. S., Peters, G. P., Enting, I. G., von Bloh, W., … Weaver, A. J. (2013). Carbon dioxide and climate impulse response functions for the computation of greenhouse gas metrics: A multi-model analysis. *Atmospheric Chemistry and Physics*, *13*, 2793–2825. https://doi.org/10.5194/acp-13-2793-2013

Khasanah, N., & van Noordwijk, M. (2018). Subsidence and carbon dioxide emissions in a smallholder peatland mosaic in Sumatra, Indonesia. *Mitigation and Adaptation Strategies for Global Change*, 1–17. https://doi.org/10.1007/s11027-018-9803-2

Kirschke, S., Bousquet, P., Ciais, P., Saunois, M., Canadell, J. G., Dlugokencky, E. J., … Cameron-Smith, P. (2013). Three decades of global methane sources and sinks. *Nature Geoscience*, *6*, 813–823. https://doi.org/10.1038/ngeo1955

Kleinen, T., Brovkin, V., von Bloh, W., Archer, D., & Munhoven, G. (2010). Holocene carbon cycle dynamics. *Geophysical Research Letters*, *37*, L02705.

Le Quéré, C., Andrew, R. M., Friedlingstein, P., Sitch, S., Pongratz, J., Manning, A. C., … Zhu, D. (2018). Global Carbon Budget 2017. *Earth System Science Data*, *10*, 405–448.

Lohila, A., Minkkinen, K., Laine, J., Savolainen, I., Tuovinen, J.-P., Korhonen, L., … Laaksonen, A. (2010). Forestation of boreal peatlands: Impacts of changing albedo and greenhouse gas fluxes on radiative forcing. *Journal of Geophysical Research*, *115*, G04011.

Mathijssen, P., Tuovinen, J. P., Lohila, A., Aurela, M., Juutinen, S., Laurila, T., … Väliranta, M. (2014). Development, carbon accumulation, and radiative forcing of a subarctic fen over the Holocene. *The Holocene*, *24*, 1156–1166. https://doi.org/10.1177/0959683614538072

Melling, L. (2013). Greenhouse gas (GHG) emission from tropical peatland. *Planter*, *89*, 725–730.

Melling, L., Goh, K. J., Kloni, A., & Hatano, R. (2012). Is the water table the most important factor influencing soil C-Flux in tropical peatland? In *Peatlands in Balance, Proceedings of the 14th International Peat Congress, International Peat Society, Stockholm, Sweden, Extended Abstract No. 330* (6 pp.).

Melling, L., Hatano, R., & Goh, K. J. (2005a). Soil CO_2 flux from three ecosystems in tropical peatland of Sarawak, Malaysia. *Tellus Series B*, *57*, 1–11. https://doi.org/10.3402/tellusb.v57i1.16772

Melling, L., Hatano, R., & Goh, K. J. (2005b). Global warming potential from soils in tropical peatland of Sarawak, Malaysia. *Phyton*, *45*, 275–284.

Miettinen, J., Hooijer, A., Vernimmen, R., Liew, S. C., & Page, S. E. (2017). From carbon sink to carbon source: Extensive peat oxidation in insular Southeast Asia since 1990. *Environmental Research Letters*, *12*, 024014. https://doi.org/10.1088/1748-9326/aa5b6f

Miettinen, J., Shi, C., & Liew, S. C. (2016). Land cover distribution in the peatlands of Peninsular Malaysia, Sumatra and Borneo in 2015 with changes since 1990. *Global Ecology and Conservation*, *6*, 67–78. https://doi.org/10.1016/j.gecco.2016.02.004

Minkkinen, K., Korhonen, R., Savolainen, I., & Laine, J. (2002). Carbon balance and radiative forcing of Finnish peatlands 1900-2100 – the impact of forestry drainage. *Global Change Biology*, *8*, 785–799. https://doi.org/10.1046/j.1365-2486.2002.00504.x

Moore, T. R., Bubier, J. L., Frolking, S., Lafleur, P., & Roulet, N. T. (2002). Plant biomass and production and CO_2 exchange in an ombrotrophic bog. *Journal of Ecology*, *90*, 25–36. https://doi.org/10.1046/j.0022-0477.2001.00633.x

Moore, T. R., de Young, A., Bubier, J. L., Humphreys, E. R., Lafleur, P. M., & Roulet, N. T. (2011). A multi-year record of methane flux at Mer Bleue Bog, Southern Canada. *Ecosystems*, *14*, 646–657. https://doi.org/10.1007/s10021-011-9435-9

Myhre, G., Shindell, D., Bréon, F.-M., Collins, W., Fuglestvedt, J., Huang, J., … Zhang, H. (2013). Anthropogenic and Natural Radiative Forcing. In T. F. Stocker, D. Qin, G.-K. Plattner, M. Tignor, S. K. Allen, J. Boschung, A. Nauels, Y. Xia, V. Bex & P. M. Midgley (Eds.) *Climate Change 2013: The Physical Science Basis. Contribution of Working Group I to the Fifth Assessment Report of the Intergovernmental Panel on Climate Change* (pp. 659–740). Cambridge, UK and New York, NY: Cambridge University Press.

Neubauer, S. C. (2014). On the challenges of modeling the net radiative forcing of wetlands: Reconsidering Mitsch et al. 2013. *Landscape Ecology*, *29*, 571–577. https://doi.org/10.1007/s10980-014-9986-1

Neubauer, S. C., & Megonigal, J. P. (2015). Moving beyond global warming potentials to quantify the climatic role of ecosystems. *Ecosystems*, *18*, 1000–1013.

Page, S. E., & Hooijer, A. (2016). In the line of fire: The peatlands of Southeast Asia. *Philosophical Transactions of the Royal Society of London. Series B, Biological Sciences*, *371*, 20150176. https://doi.org/10.1098/rstb.2015.0176

Page, S. E., Rieley, J. O., & Banks, C. J. (2011). Global and regional importance of the tropical peatland carbon pool. *Global Change Biology*, *17*, 798–818. https://doi.org/10.1111/j.1365-2486.2010.02279.x

Pangala, S. R., Moore, S., Hornibrook, E. R., & Gauci, V. (2013). Trees are major conduits for methane egress from tropical forested wetlands. *New Phytologist*, *197*, 524–531. https://doi.org/10.1111/nph.12031

Petrescu, A. M. R., Lohila, A., Tuovinen, J.-P., Baldocchi, D. D., Desai, A. R., Roulet, N. T., … Cescatti, A. (2015). The uncertain climate footprint of wetlands under human pressure. *Proceedings of the National Academy of Sciences*, *112*, 4595–4599.

Ritz, S. P., Stocker, T. F., & Joos, F. (2011). A coupled dynamical ocean–energy balance atmosphere model for paleoclimate studies. *Journal of Climate*, *24*, 349–375. https://doi.org/10.1175/2010JCLI3351.1

Roulet, N. T. (2000). Peatlands, carbon storage, greenhouse gases, and the Kyoto Protocol: Prospects and significance for Canada. *Wetlands*, *20*, 605–615. https://doi.org/10.1672/0277-5212(2000)020[0605:PCSGGA]2.0.CO;2

Roulet, N. T., Lafleur, P. M., Richard, P. J. H., Moore, T. R., Humphreys, E. R., & Bubier, J. L. (2007). Contemporary carbon balance and late Holocene carbon accumulation in a northern peatland. *Global Change Biology*, *13*, 397–411. https://doi.org/10.1111/j.1365-2486.2006.01292.x

Stocker, B. D., Roth, R., Joos, F., Spahni, R., Steinacher, M., Zaehle, S., … Prentice, I. C. (2013). Multiple greenhouse-gas feedbacks from the land biosphere under future climate change scenarios. *Nature Climate Change*, *3*, 666–772. https://doi.org/10.1038/nclimate1864

Sumawinata, B., Suwardi, & Munoz, C. P. (2012). Emission of CO_2 and CH_4 from Plantation Forest of Acacia crassicarpa on peatlands in Indonesia. Extended Abstract No 114. In *Proceedings of the 14th International Peat Congress, Stockholm* (pp. 1–6).

Van der Werf, G. R., Morton, D. C., DeFries, R. S., Olivier, J. G., Kasibhatla, P. S., Jackson, R. B., … Randerson, J. T. (2009). CO_2 emissions from forest loss. *Nature Geoscience*, *2*, 737–738. https://doi.org/10.1038/ngeo671

Verwer, C., & van der Meer, P. (2010). *Carbon pools in tropical peat forest – Towards a reference value for forest biomass carbon in relatively undisturbed peat swamp forests in Southeast Asia. Alterra-report 2108* (64 pp). Wageningen: Alterra.

Whiting, G. J., & Chanton, J. P. (2001). Greenhouse carbon balance of wetlands: Methane emission versus carbon sequestration. *Tellus*, *53B*, 521–528.

Wijedasa, L. S., Jauhiainen, J., Könönen, M., Lampela, M., Vasander, H., Leblanc, M. C., … Andersen, R. (2017). Denial of long-term issues with agriculture on tropical peatlands will have devastating consequences. *Global Change Biology*, *23*, 977–982. https://doi.org/10.1111/gcb.13516

Wilson, D., Blain, D., Couwenberg, J., Evans, C. D., Murdiyarso, D., Page, S. E., … Tuittila, E. S. (2016). Greenhouse gas emission factors associated with rewetting of organic soils. *Mires and Peat*, *17. Article*, *04*, 1–28.

SUPPORTING INFORMATION

Additional supporting information may be found online in the Supporting Information section at the end of the article.

How to cite this article: Dommain R, Frolking S, Jeltsch-Thömmes A, Joos F, Couwenberg J, Glaser PH. A radiative forcing analysis of tropical peatlands before and after their conversion to agricultural plantations. *Glob Change Biol*. 2018;24:5518–5533. https://doi.org/10.1111/gcb.14400